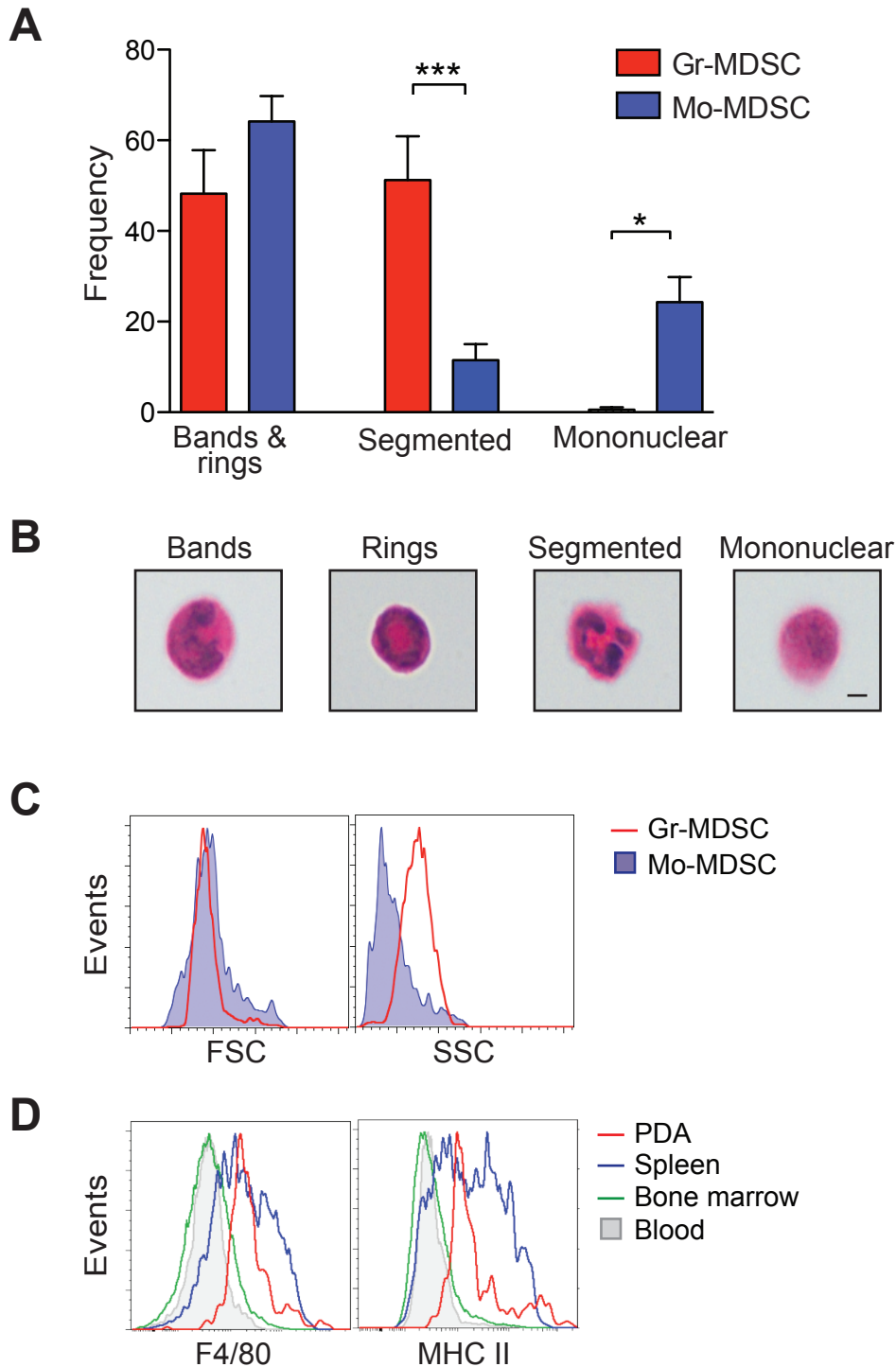
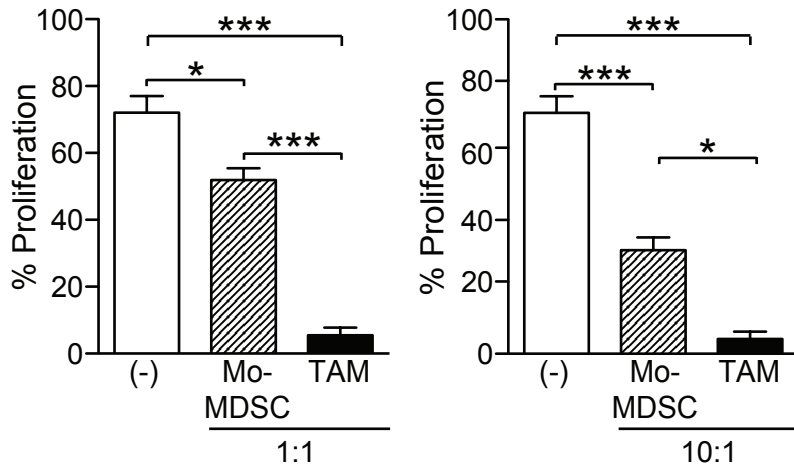
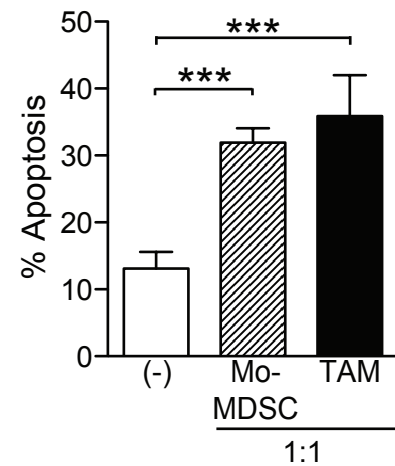


Supplementary Figure 1. Cancer-conditioned myeloid cells are increased in tumor-draining (PDA) vs. normal lymph nodes. Draining lymph nodes (dLN) were dissected from normal pancreas or from *KPC* mice with PDA and single cell suspensions stained for CD45 to confirm a lack of contamination from non-lymphoid tissue (top). Representative CD45+ gated FACS profiles reveal an increase in myeloid subsets in PDA dLN compared to normal pancreatic dLN (bottom).



Supplementary Figure 2. Morphological spectra of cancer-conditioned myeloid subsets. (A) Quantitative analysis of nuclear morphology of sorted splenic Gr-MDSC and Mo-MDSC subsets stained with Wright Giemsa. 6 to 8 high-powered fields from slides of 2 independent preparations were analyzed. ***, $p=0.0004$; *, $p=0.0054$. (B) Representative images of distinct MDSC nuclear morphologies quantified in (A). Scale bar, 1 μm . (C) Representative histograms for size (FSC) and granularity (SSC) of MDSC subsets. (D) Expression of maturation/differentiation markers on Gr-MDSC isolated from the indicated tissues.

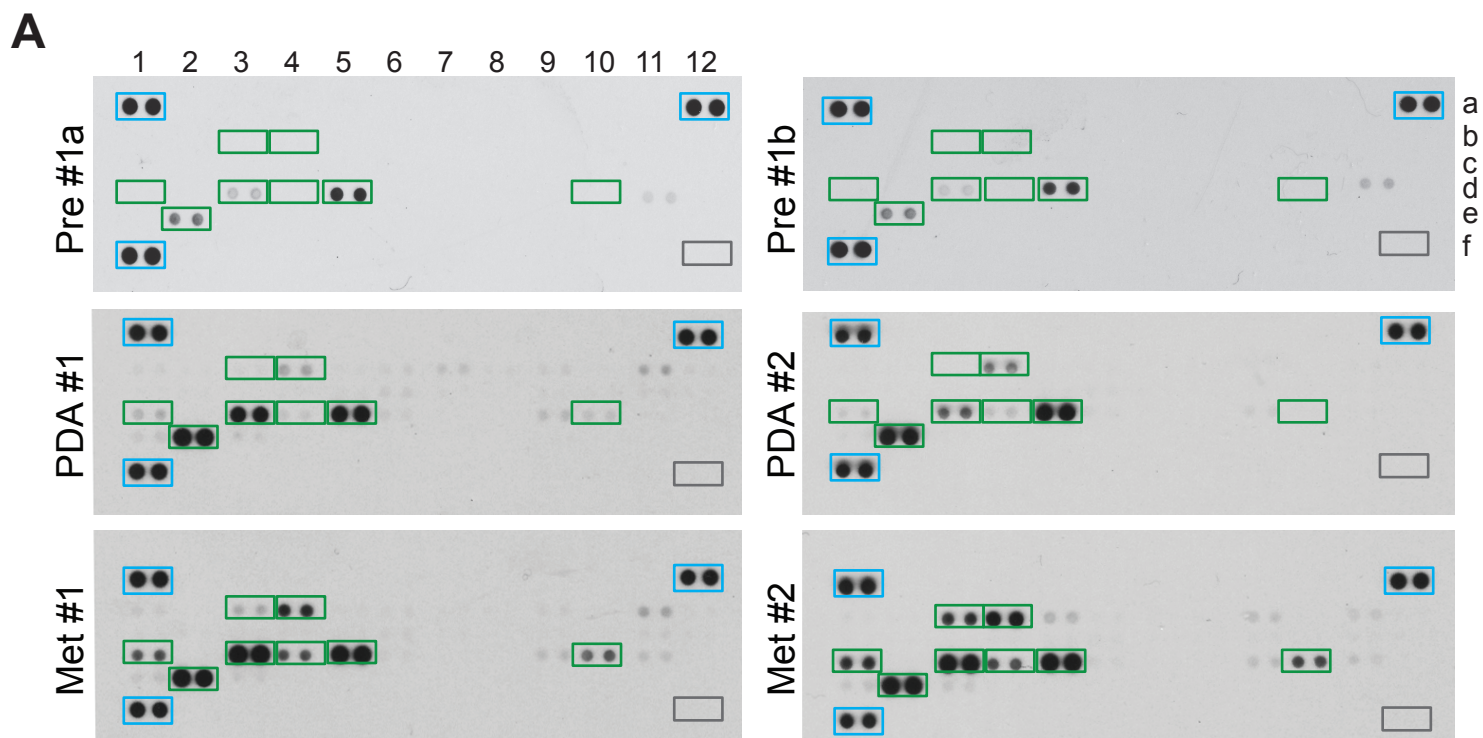
A**B**

Supplementary Figure 3. Mo-MDSC and TAM isolated from *KPC* mice with PDA are immunosuppressive.

(A) Naive T cell proliferation in response to anti-CD3/CD28 is significantly suppressed by Mo-MDSC and TAM both at a 1:1 and 10:1 myeloid cell to T cell ratio. Graphs indicate the percentage of CD8 T cells that have undergone cell division at 48h.

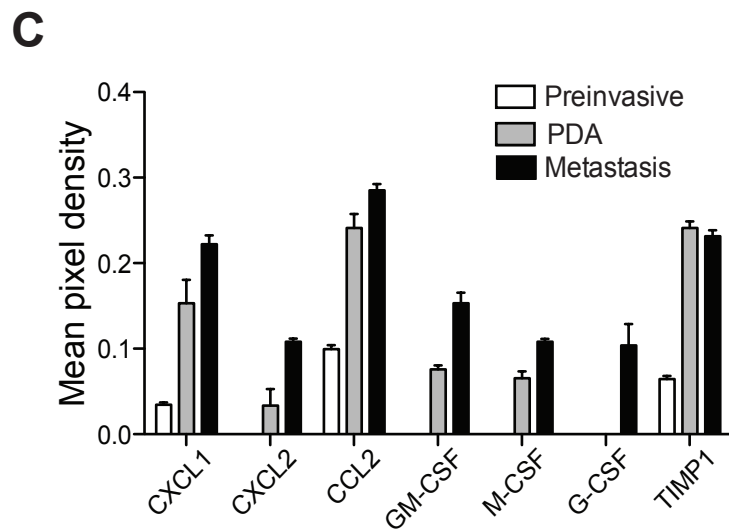
(B) Mo-MDSC and TAM induce CD8 T cell apoptosis. Graph indicates the percentage of CD8+ Annexin-V+ T cells after stimulation in the presence or absence (-) of purified myeloid subsets.

Data represent mean \pm SEM from 4 independent experiments. Statistical significance was determined using a one-way ANOVA and a Tukey's post test to correct for multiple comparisons.



B

1	2	3	4	5	6	7	8	9	10	11	12
REF											REF
CXCL13	C5/C5a	G-CSF	GM-CSF	CCL1	Eotaxin	sICAM-1	IFN-g	IL-1a	IL-1B	IL-1Ra	IL2
IL-3	IL-4	IL-5	IL-6	IL-7	IL-10	IL-13	IL-12 p70	IL-16	IL-17	IL-23	IL-27
CXCL19	CXCL11	CXCL1	M-CSF	CCL2	CCL12	CXCL9	CCL3	CCL4	CXCL2	CCL5	CXCL12
CCL17	TIMP1	TNF-a	TREM-1								
REF											Negative

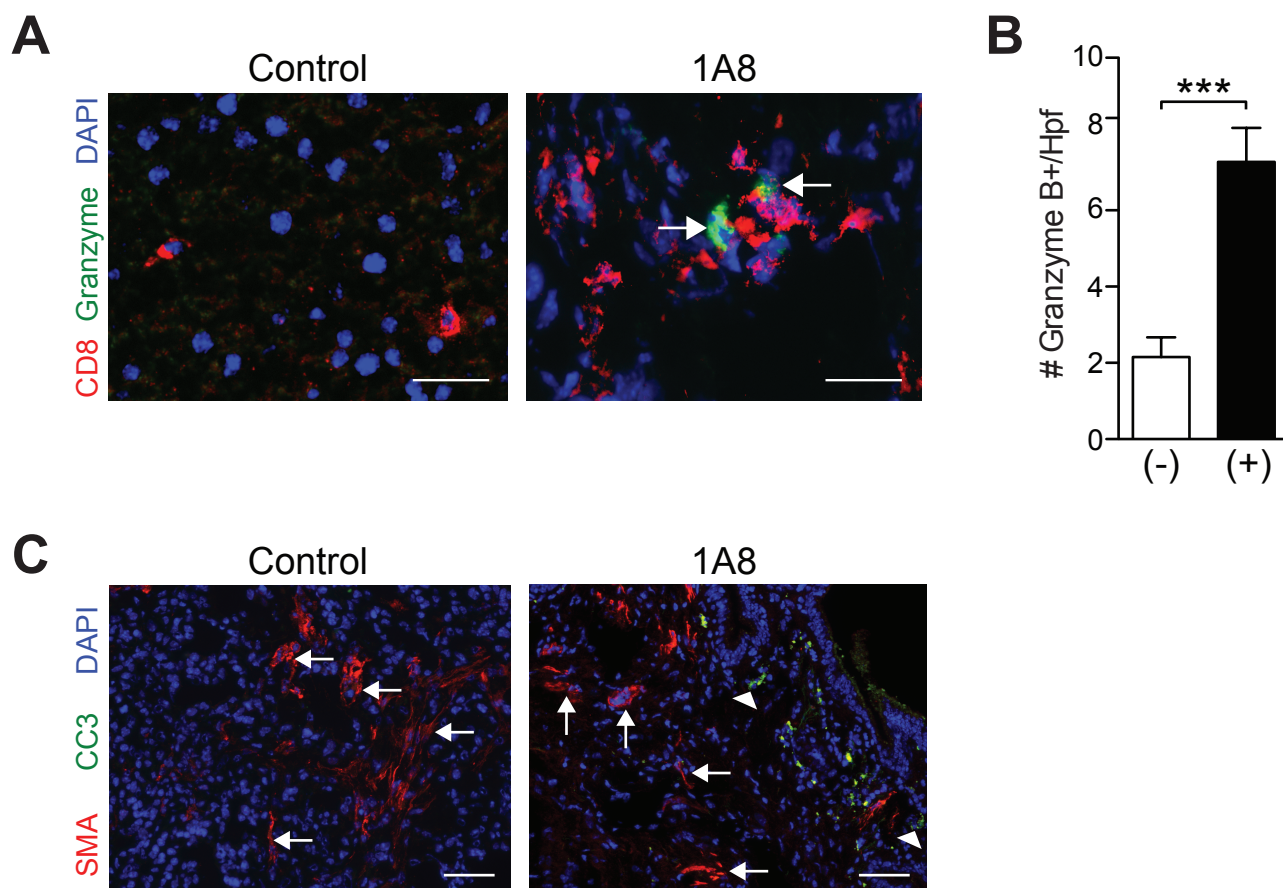


Supplementary Figure 4. Preinvasive and invasive PDA cell secretome.

(A) Expression of proteins in preinvasive epithelial cells (top row), and two independently derived primary tumor cells and their paired metastatic cells. Green boxes indicated proteins expressed in ≥ 2 invasive cell samples, blue boxes indicate internal reference control, and gray boxes indicate negative controls.

(B) Map for protein arrays in (A).

(C) Mean pixel density of arrays in (A).



Supplementary Figure 5. Gr-MDSC depletion promotes CD8 T cell degranulation but does not impact stromal cell apoptosis.

(A) Compound immunofluorescence for CD8 T cells, granzyme B (arrows), and DAPI in PDA from untreated (control) or 1A8-treated *KPC* mice.

(B) Quantification of granzyme B+ cells per high power field (Hpf).

(C) Compound immunofluorescence for the pancreatic stellate cell activation marker α SMA (arrows), cleaved caspase-3 (CC3) (arrowheads), and DAPI in PDA from control or 1A8-treated *KPC* mice. Scale bar, 50 μ m.